Palaeogeography, Palaeoclimatology, Palaeoecology 415 (2014) 59–68

Contents lists available at ScienceDirect

Palaeogeography, Palaeoclimatology, Palaeoecology

journal homepage: www.elsevier.com/locate/palaeo

Understanding Holocene variations in the vegetation of Sao Joao River basin, southeastern coast of Brazil, using phytolith and carbon isotopic analyses

Heloisa H.G. Coe [a], Kita Macario [b,*], Jenifer G. Gomes [a,b], Karina F. Chueng [a], Fabiana Oliveira [b], Paulo R.S. Gomes [b], Carla Carvalho [b,c], Roberto Linares [b], Eduardo Alves [b], Guaciara M. Santos [d]

[a] Universidade do Estado do Rio de Janeiro, São Gonçalo, RJ, Brazil
[b] Universidade Federal Fluminense, Niteroi, RJ, Brazil
[c] Universidade do Estado do Rio de Janeiro, Rio de Janeiro, RJ, Brazil
[d] University of California, Irvine, CA, United States

ARTICLE INFO

Article history:
Received 31 May 2013
Received in revised form 9 January 2014
Accepted 18 January 2014
Available online 25 January 2014

Keywords:
Radiocarbon
Phytolith
^{14}C-AMS

ABSTRACT

To understand variations in the vegetation of the southeastern coast of Brazil during the Holocene and to identify roughly when they took place, we make use of phytolith morphology and carbon stable isotope analyses coupled with ^{14}C dating of soil profiles. The soil profile studied is located in the Sao Joao River Basin close to Cabo Frio, Rio de Janeiro State. We evaluated the soil characteristics, which showed great variations in granulometry, with larger texture in upper horizons that enabled the movement of particles to lower layers. The accumulation soil horizons revealed several palaeoclimatic aspects: higher phytolith stocks, a higher density of trees, and a lower water stress at the bottom of the profile, and a predominance of C3 grasses throughout the Holocene. Carbon stable isotopic ratios of the soil profile confirm the predominance of C3 plants, except for E/Bt horizon which was enriched in ^{13}C. The soil organic matter mean residence time ranges from post-bomb (topsoil) to 10,245 years cal BP at the base of the profile. The results of this study are compatible with other evidence of a more humid environment in the first half of the Holocene.

1. Introduction

The Brazilian Southeast was formerly occupied by Atlantic forest before the arrival of Europeans in the 16th century, when deforestation slowly started to take place. This region has undergone important climatic oscillations during the Quaternary (e.g. Ledru et al., 1998; Marchant and Hooghiemstra, 2004; Cruz et al., 2005, 2006; Wanner et al., 2008; Wanner and Brönnimann, 2012; Buso et al., 2013).

The Sao Joao River basin, originally within the Atlantic forest biome, is an area that is still poorly studied in terms of its landscape and soil profile evolution. Although most of the original Atlantic forest vegetation has been lost, some information can still be obtained from the study of phytoliths deposited in soil layers.

Phytoliths are microscopic particles formed as a result of absorption of dissolved silicon (Si) from soils by roots, followed by deposition and biomineralization. These biosilica structures can be found inside the cells of many living plants. Furthermore, they are usually found within the finest sand fractions, where the whole plant or tissue parts have decayed (Piperno, 1988). After being recovered from soils, these microfossils show configurations that can be associated with their original vegetation. Phytoliths can be classified by taxonomy or by their physical characteristics, and they are generally studied by analyses of their assemblages.

After phytolith morphotypes are identified, calculation of phytolith indices helps track some important environmental parameters, such as density of trees, adaptation to drought, or water stress (Fredlund and Tieszen, 1994; Bremond et al., 2005a,b; Messager et al., 2010; Coe et al., 2012). Even though some phytoliths can percolate downwards through the soil profile, statistical analysis of phytolith assemblages can still provide valuable information on the vegetation patterns. As Krauss et al. (1997) pointed out, as long as the soil composition is relatively uniform with depth, it is safe to assume that the percolation rate for a given phytolith morphotype will not vary significantly.

Stable isotopes of carbon (^{12}C and ^{13}C) can also be used as a proxy of biological processes in plants. Carbon isotopic discrimination during photosynthesis provides insight into photosynthetic

* Corresponding author. Tel.:+55 2126 295 892.
E-mail address: kita@mail.if.uff.br (K. Macario).

0031-0182/$ – see front matter © 2014 Elsevier B.V. All rights reserved.
http://dx.doi.org/10.1016/j.palaeo.2014.01.009

metabolism in plants as well as its environmental influences. For instance, plants that utilize the Calvin–Benson photosynthetic pathway, which tends to prefer the lighter isotope, are referred to as C3 and have $\delta^{13}C$ values from −32 to −22‰. The C4 plants use the Hatch–Slack cycle and have $\delta^{13}C$ values in the range of −9 to −17‰ (Gleixner, 2002; Gordon and Goñi, 2003; Killops and Killops, 2005). Consequently, the $^{13}C/^{12}C$ ratio in soil organic matter (SOM) should remain close to the ratio of the original vegetation. However, due to organic matter (OM) heterogeneity in soils and sediments, $\delta^{13}C$ values will depend on the OM original sources (Hedges and Parker, 1976). In forest ecosystems $\delta^{13}C$ values of soil OM (SOM) are generally less negative than the source vegetation. Studies show an increase of 1 or 2‰ during decomposition of vegetable tissues (Martinelli et al., 2009).

Information regarding palaeovegetation changes can ultimately be related to its possible time of occurrence by radiocarbon (^{14}C) dating of SOM. Although charcoal fragments and humin are the most appropriate fractions for dating SOM (Pessenda et al., 2001), the lack of sufficient amounts in some cases has been forcing researchers to rely on ^{14}C dates obtained on total SOM. Because SOM is composed of a complex mixture of OM of different origins in various stages of decomposition, its age is normally significantly younger than dates obtained from more stable organic compounds found in soil (Pessenda et al., 2001). Therefore, its bulk ^{14}C age can only represent a mean residence time (MRT) of the OM in the soil sample (Martin and Johnson, 1995) and should be interpreted with caution. Because the pool of OM in some soils can also be very scarce, MRT is normally obtained by the ^{14}C method performed by the accelerator mass spectrometry (AMS) technique. The MRT ages of SOM are then assumed to be the minimum mean ages of phytolith assemblage deposition in these soils.

In order to better understand the variations in the vegetation of Sao Joao River basin during the Holocene, we performed phytolith and carbon stable isotope analyses coupled with ^{14}C dating of total SOM samples.

2. Study area

The Sao Joao River basin is located between 22°20′ and 22°50′ S and 40°00′ and 42°40′ W, covering a surface of 2160 km^2 and a perimeter of 266 km. Eight counties constitute the basin: Cachoeiras de Macacu, Rio Bonito, Casimiro de Abreu, Araruama, Sao Pedro da Aldeia, Cabo Frio, Rio das Ostras and Silva Jardim (Bidegain, 2005) (Fig. 1).

This region features a humid tropical climate, with precipitation concentrated during the summer (average annual rainfall of 2000 mm) and a mean annual temperature of 25.5 °C (Cunha, 1995).

In the past, the region was covered by a lowland rain forest with high altitude grasslands lining the mountains, the plateau and the hills. However, continuous deforestation for logging and/or farming reduced the long and continuous extension of tropical forest to isolated fragments of vegetation surrounded by areas of agriculture. The current basin landscape consists mostly of cleared fields and secondary forests, alluvial forests, and forested hills. Nowadays, the land in the basin is subdivided for use as cities, farmland, and pastures, and it contains different types of vegetation, such as forests, swamps, altitude fields,

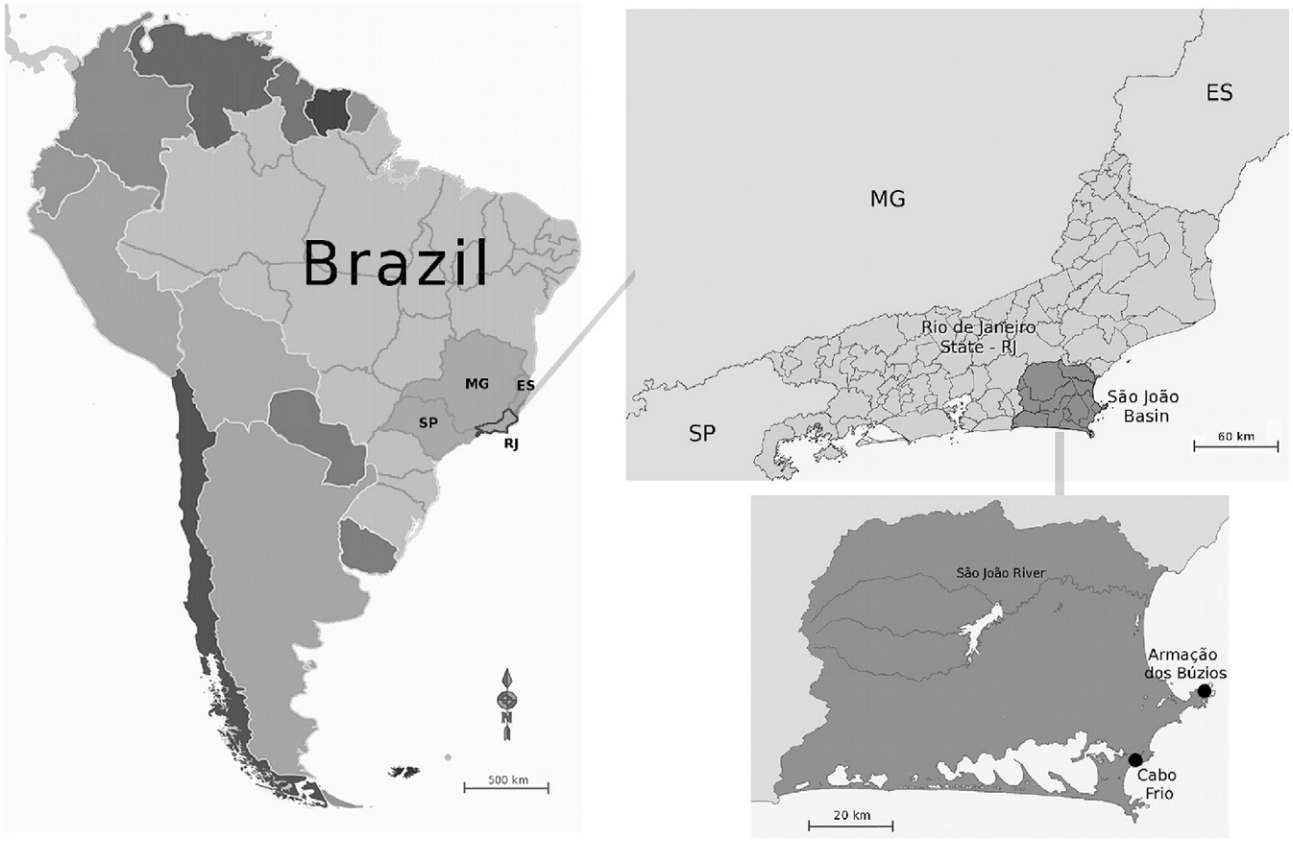

Fig. 1. Sao Joao hydrographic basin map, with cities.
Source: modified from Consórcio Intermunicipal Lagos São João, 1999) in http://www.micoleao.org.br/arquivos/mapas/bacia_sao_joao.jpg.

flooded fields, pastures and "restingas" (Quintela and Cunha, 1990) (Fig. 2).

The topography of the basin is predominantly of coastal plains and also some mountains, hills, plateaus, lowland areas that are subject to continuous or periodic flooding, and sandbanks. The most common soils of this region are classified as red-yellow oxisols, cambisols, gleysols, histosols and fluvisols (Primo and Volker, 2003).

3. Materials and methods

3.1. Sites and samples

To provide modern references for interpreting fossil phytolith assemblages, samples were collected from soils just below the litter of the main types of current vegetation in Sao Joao River Basin: mangrove (one sample of Rizophora and another of Langucularia); forest (with or without the presence of palm trees), grasses, pasture, and marsh. In total, seven modern assemblages (MA) were collected (Fig. 2).

The studied soil profile is from a lowland coastal plain in the county of Cabo Frio (coordinates 22°49′55.54″ S, 42°00′53.85″ W; represented by a triangle in Fig. 2), less than 5 m above sea level. It is a planesol with the following horizons: A: 0–15 cm depth; E: 15–45 cm depth; E/Bt: 45–90 cm depth and Bt: 90–140 cm (Fig. 3). At present, its vegetative cover is composed of grasses.

For soil profiles showing distinguishable horizons with well-defined characteristics, any sub-sample should be representative of the whole horizon in terms of granulometry, color and mineralogical composition. Although many environmental reconstruction studies are based on continuous sampling (usually from each 10 cm, ignoring the horizon definition), other works have shown that horizon-based sampling can be also representative (Kelly et al., 1998; Sedov et al., 2003; Tapia et al., 2003; Borrelli et al., 2006; Bement et al., 2007; Coe, 2009).

For each horizon, a large amount of sample (about 10 cm thick) was collected from the deepest part of the horizon, close to the transition to the next horizon. The depths of the samplings were: Horizon A: 5–15 cm; Horizon E: 35–45 cm; Horizon E/Bt: 80–90 cm; Horizon Bt: 110–120 cm. Then, about 20 g of soil was

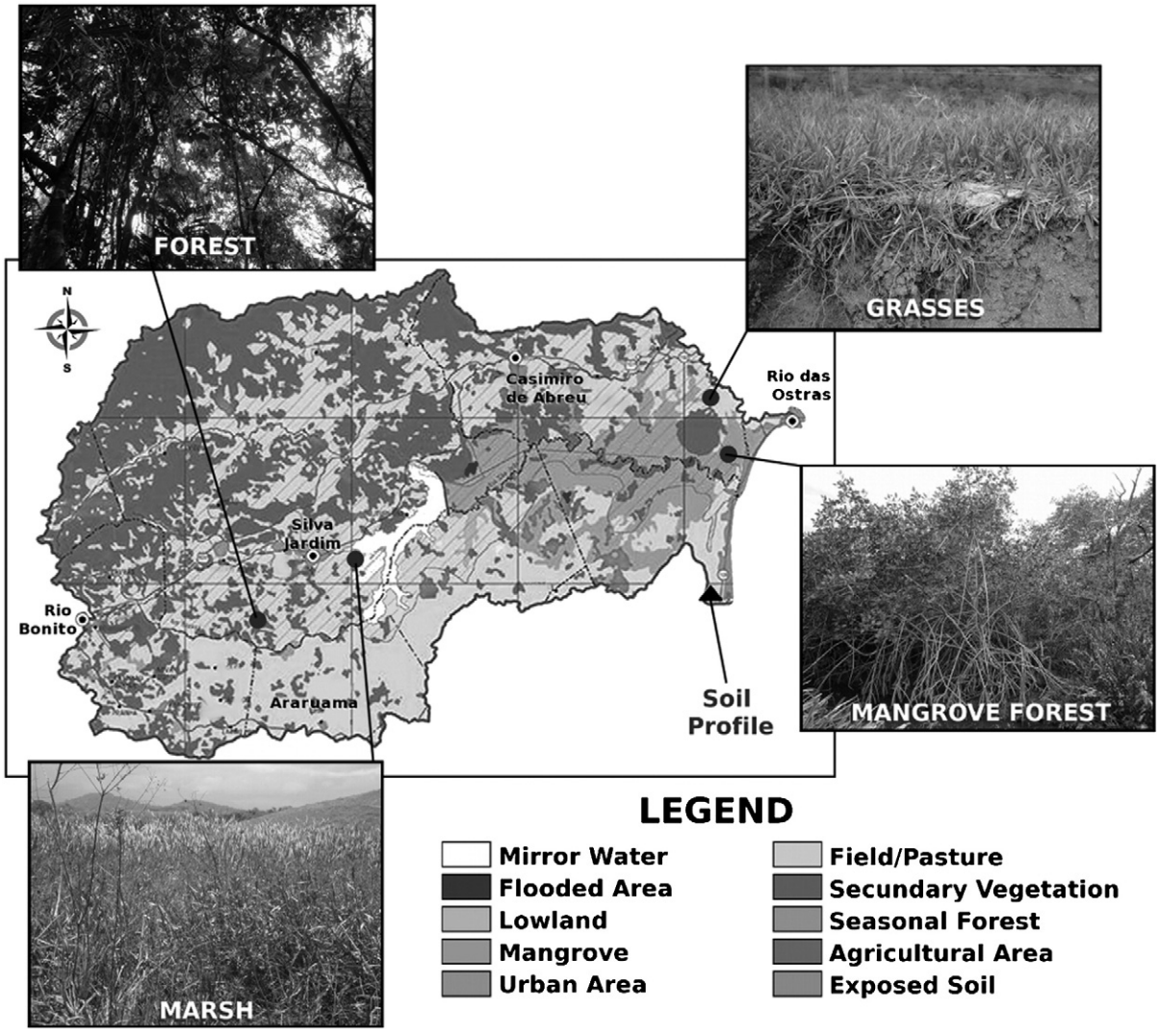

Fig. 2. Areas from where modern assemblages (MA) and the soil profile were collected in Sao Joao river basin.
Source: modified from Consórcio Intermunicipal Lagos São João, 1999) in http://www.micoleao.org.br/arquivos/mapas/bacia_sao_joao.jpg.

homogenized and subdivided into small aliquots to undergo phytolith analyses.

3.2. Methods

3.2.1. Soil granulometry

The soil analyses were performed at the Laboratory of Physical Geography (LAGEFIS) — UERJ. For each sample, a particle size analysis was done. These analyses were carried out using the EMBRAPA pipette method. The soil texture was obtained using the Triangle American Textural Classes, described by the Soil Survey Manual and modified by the Brazilian Society of Soil Science (Saraiva, 2012).

3.2.2. Phytolith analyses

3.2.2.1. Chemical extraction and counting. Phytoliths were extracted from 20 g of dry soil, slightly crushed, sieved at 2 mm, and processed through the following stages (Kelly, 1990): (1) dissolution of carbonates using HCl (1 N); (2) oxidation of organic matter using H_2O_2 (30%) at 90 ºC; (3) solubilization of iron oxides using sodium citrate ($Na_3C_6H_5O_7$) and sodium hydrosulfite ($Na_2S_2O_4$); (4) removal of the clay fraction (<2 mm) by decantation; (5) densimetric separation of opal particles in a heavy liquid of sodium polytungstate (density of 2.3 g/cm^3). Particles were dried and weighed after extraction. Phytoliths were then mounted on microscope slides in glycerin for 3D observation and in Entellan for counting at 400× magnification. At least 200 phytoliths with taxonomic significance were counted.

3.2.2.2. Phytolith types. Phytoliths were classified following the morphological classification schemes of Twiss (1992) and Twiss et al. (1969). These were improved and completed by phytolith shape descriptions in Mulholland (1989), Fredlund and Tieszen (1994), Kondo et al. (1994), Alexandre et al. (1997b); Strömberg (2004), Mercader et al. (2009), and named after the International Code for Phytolith Nomenclature 1.0 (Madella et al., 2005). Phytoliths without taxonomic significance because of their dissolution or fragmentation were gathered into an unclassified category. Types are presented as percentages of the sum of classified phytoliths.

3.2.2.3. Phytolith indices. Three phytolith indices were calculated as follows: (1) the D/P index is the ratio of the dicotyledonous phytolith type (globular granulate) over the sum of Poaceae phytolith types (short cells, acicular and bulliform) (Bremond et al., 2005a); (2) the hydrous stress index Bi, previously named Fs (Bremond et al., 2005b; Messager et al., 2010) is the ratio of the bulliform type over the sum of Poaceae phytolith types, expressed as a percentage; and (3) the aridity index Iph (Fredlund and Tieszen, 1994; Bremond et al., 2005b) is the ratio of bilobate type over the sum of short cells phytolith types.

3.2.3. Stable isotope analyses

Isotopic analyses of carbon were performed by the Laboratory of Isotope Ecology of CENA/USP. Because the carbonate fraction in the studied soil was found to be negligible, measurements were performed on bulk samples. The samples were weighed in tin capsules using an analytical balance. The analyses of the elemental composition of OM concentrations were carried out in a Carlo Erba elemental analyzer model EA 1110 coupled to a mass spectrometer Finnigan Delta Plus, allowing the simultaneous determination of organic carbon concentration and isotope signatures. Results are expressed as $\delta^{13}C$ relative to PDB (Pee Dee Belemnite) defined as $\delta^{13}C$ (‰ — parts per thousand) = ([R sample / R standard] − 1) × 1000. The samples were analyzed with a precision of 0.2‰. The limit of detection for C was 0.03%.

3.2.4. Radiocarbon analyses

Radiocarbon sample processing and analyses were performed at two facilities; the Radiocarbon Laboratory at the Fluminense Federal University (LAC-UFF) in Niteroi, RJ, Brazil, and at the Keck-CCAMS Facility at University of California, Irvine, USA (KCCAMS/UCI).

Most of the total SOM ^{14}C-AMS measurements were performed at LAC-UFF, which runs a NEC 250 kV Single Stage Accelerator Mass Spectrometry system. Before measurements, the SOM fraction was chemically separated using 1 N HCl at 90 °C to remove carbonates. This procedure was repeated until the samples stop foaming and the supernatant was clear, after which the SOM fraction was rinsed with deionized water to neutral pH and dried at 90 °C. Pretreated samples were then combusted in sealed evacuated prebaked quartz tubes at 900 °C, cryogenically cleaned, and converted to graphite using zinc and titanium hydrate, with iron catalyst in Pyrex tubes in a muffle oven at 520 °C for 7 h as described in Xu et al. (2007).

In order to verify the distribution of ^{14}C ages of different chemical soil fractions (Pessenda et al., 2001), a refractory C fraction (humin) was extracted from the topsoil horizon, following the conventional acid–base–acid (ABA) protocol (Santos and Ormsby, in press). The ABA pre-treatment can be summarized as repeated baths with 1 N HCl and 1 N NaOH at ~70 °C, with the base washes repeated until the extract labile humic acid is fully removed. Upon pretreatment, clean samples were combusted to CO_2, cryogenically cleaned, and reduced to graphite by hydrogen reduction following established protocols (Santos et al., 2007a,b). This procedure and ^{14}C-AMS measurement was carried out at UCI, as we anticipated that the graphite target with a very low carbon mass (<<0.050 mgC) would be produced. The KCCAMS/UCI facility runs a modified NEC 0.5MV 1.5SDH-2 AMS system, allowing it to measure graphite samples of 0.010 mgC with 1% precision when regular targets are measured at 0.2–0.3% precision for modern carbon samples (Beverly et al., 2010). Duplicates of all soil horizons, except E, were also ^{14}C-AMS measured at UCI for comparison. Carbonates were removed from soil, using just 1 N HCl rinses as described earlier.

All ^{14}C results were corrected using the on-line $\delta^{13}C$ AMS values of the respective graphite aliquots measured obtained during the respective ^{14}C-AMS measurements by both facilities. Control and background samples, subjected to the same chemical procedures as unknown samples, were also processed to graphite and measured.

Age calibrations were performed using CalibBomb (http://calib.qub.ac.uk/CALIBomb/) and the Southern Hemisphere (SHCal04) dataset (McCormac et al., 2004) in the OxCal4 software (Bronk Ramsey, 2009).

4. Results

4.1. Phytolith analyses

We evaluated the soil characteristics, which presented great variations in granulometry and thick texture in the top horizons (A and E). These horizons are extremely sandy (>86%), enabling particles (including phytoliths) to move downward to the lower layers. From E/Bt to Bt horizons the proportion of clay increased up to 54%, reflecting the accumulation of material from higher horizons (Table 1 and Fig. 3). The results of the phytolith assemblages and the isotopic and grain size analyses allowed us to distinguish two zones in the soil profile. A lower one, the Bt horizon (now called Zone I), and another encompassing the upper horizons E/Bt, E and A (Zone II) (Table 1 and Figs. 3, 4 and 5).

Phytolith stock was high (between 2.7 and 2.5%) and does not show the usual trend of diminishing with depth (Alexandre et al., 1997a). Its concentration remains fairly constant (2.6%; n = 3)

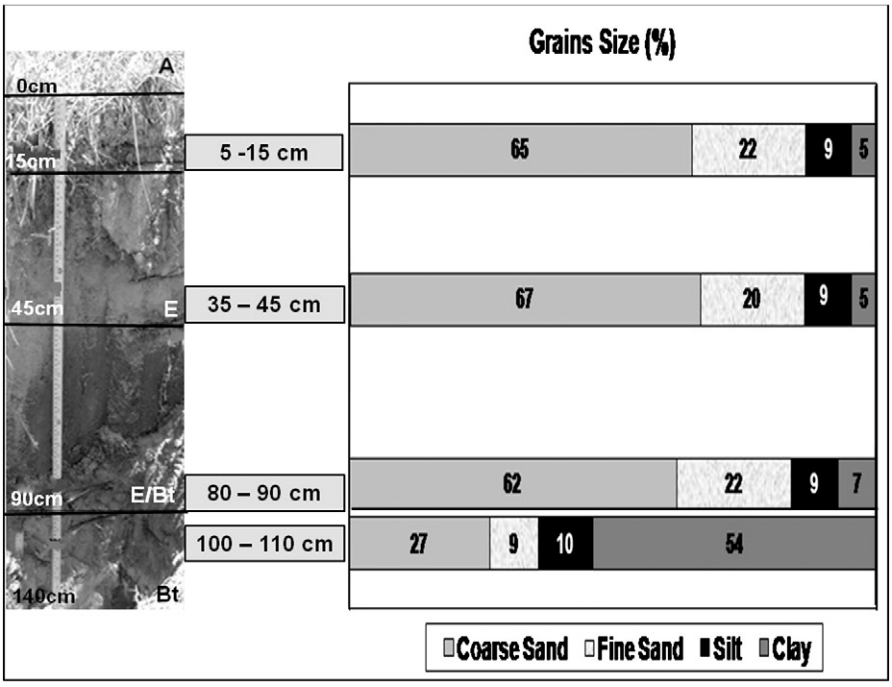

Fig. 3. Studied soil profile with its horizons, sampling depths and grain size.

within the upper three horizons (Zone II) and doubles (5%) in the bottom horizon (Zone I) as shown in Fig. 5. A similar increase in the stock of phytoliths has been reported by Coe et al. (2012) in soil profiles in Búzios (approximately 20 km north of the present studied area) and also within Rio de Janeiro State (Fig. 1), where field and petrographical observations, as well as C/N and phytolith concentration values, suggest the occurrence of three phases of soil development, indicated by the occurrence of a buried humic horizon, followed by an erosive phase, materialized by a petrographical discontinuity.

In contrast to the findings of Coe et al. (2012), however, no evidence of colluviation or any other type of lithological discontinuity was detected in the present soil profile. Moreover, the granulometry of the present soil profile follows the same zone division of the phytolith zones. These factors may explain the relatively good correlation between the increased stock of phytoliths (2.5 to 5%) and the percentage of finer soil fractions (silt and clay; from about 14% to 64%) in the bottom horizon (Fig. 3).

Among the observed phytolith particles, most could be classified. However, the amount of classified phytoliths decreased sharply with depth, as the deeper ones tend to be older and consequently less preserved as a consequence of longer exposure time to weathering processes.

Phytoliths were predominantly from grass types (>70% in all horizons). This large percentile was from phytoliths formed into larger cells, such as polyhedral bulliform (from 33 to 44%), elongate (from15 to 6%), and bulliform cuneiform (from 6 to 8%). Short cells phytoliths constitute just 9% to 12%. The globular granulate phytolith showed a significant decrease from Zone I (14%) to Zone II (6 to 8%). Fig. 4 shows the types of classified phytoliths by depth.

Horizon Bt contains a lower fraction of bulliform phytoliths, which are generally adapted to water stress. Moreover, this horizon shows an increased fraction of globular granulate and globular echinate phytoliths. These forms are characteristic of woody and palm trees, which are normally more adapted to humid climates. They cannot be a product of percolation of biosilica from the upper layers, as the percentages in these layers are much lower from A to E/Bt (Table 1 and Fig. 4). In addition, due to their morphology and large size, these kinds of phytoliths tend to percolate less easily from the top layers than the smaller ones, such as the short cells (Alexandre et al., 1997a). Hence, we conclude that their presence in this horizon must be from direct deposition from the original vegetation source.

The phytolith index D/P (density of trees) exhibits values characteristic for open vegetation for most of the profile (between 0.1 and 0.2), increasing in the deepest horizon possibly due to increased humidity. In tropical Africa, Barboni et al. (1999) found similar D/P values in shrubland, grassland and semi-desert grassland areas, and Bremond et al. (2005a,b) for shrub and tall savanna and woodland. In Brazil, Alexandre et al. (1999) found D/P values between 0.3 and 0.8 for the cerrado vegetation of Minas Gerais (MG) (Fig. 1) and concluded that they are associated with open vegetation with trees and shrubs. Calegari (2009) found values between 0.4 and 0.6 for the Salinas region, also in Minas Gerais under cerrado vegetation. Coe (2009), while studying a xeric vegetation in Búzios, Rio de Janeiro (Fig. 1), found values between 0.1 and 0.8.

The short cell phytoliths are not significant (just 9% in the E horizon to 12% in the A horizon), restricting the interpretation of the Iph index (drought). The Iph index shows a peak in the E/Bt horizon (40%) and has its lowest value in horizon E (8.6%). In Africa, Bremond et al. (2005b) found that high Iph values (>20–40%) record grasslands dominated by Chloridoideae, i.e. xerophytic short grass savannas, and hence the prevalence of warm and dry climate conditions. Conversely, low Iph values (<20–40%) indicate associations in which Panicoideae, i.e. mesophytic C4 grasses, dominate, suggesting a warm and humid climate and/or high availability of soil moisture. However, local association of perennial Panicoideae grasses with annual Chloridoideae may occur in Saharan desert zones (Bremond et al., 2005b). Here, the general trend suggests a predominance of C3 plants.

Table 1
Phytolith concentration, phytolith types, phytolith indices D/P and Bi, carbon content, isotopic results and grains size analyses.

Horizon	Sampling depth[a]	TOC[b]	Phytolith amount[c]	Paral. bulliform[d]	Cuneiform bulliform[d]	Blocky[d]	Elongate[d]	Acicular[d]	Gl. granulate[d]	Gl. echinate[d]	Bilobate[d]	Saddle[d]
A	10	1.1	2.6	33	15	19	10	5	6	1	3	3
E	40	0.5	2.3	42	6	16	16	3	8	1	5	1
E/Bt	85	0.42	2.6	44	7	11	13	6	7	1	0	4
Bt	115	0.66	4.8	37	7	2	10	13	14	5	3	3

[a] In cm.
[b] In %.
[c] In % of dry weight <2 mm.
[d] In % of the sum of classified phytoliths.
[e] In % of counted particles.
[f] In ‰.

The Bi (or Fs) index (water stress) as used by Bremond et al. (2005b) in Africa provided useful reference values that are associated with desert and woodland (15.8) and forest tall grass savanna (6.29). By comparison, our Bi index values, which are higher in Zone II and lower in Zone I, suggest that the climate was more humid toward the base of the soil profile. Table 1 and Fig. 5 show the index values against depth.

4.2. Total organic carbon (TOC) and isotopic analyses

The TOC values range from 1.1% (A horizon) to 0.4. Values decrease with depth, except in Zone I, where the value increases to 0.7 (Table 1 and Fig. 5). This increase may be due to the fact that this is a textural horizon having more than 50% clay, a texture in which organic matter typically accumulates.

No significant isotopic differences with depth are observed in the soil profile studied here (Table 1). Overall, the $\delta^{13}C$ values ranged narrowly from −23.7‰ in the surface to −22.1‰ in Bt horizon, suggesting the presence of C3 vegetation (Boutton, 1991; Desjardins et al., 1996; Pessenda et al., 1996, 1998). The $\delta^{13}C$ increase of 1.6‰ with depth could be due to isotope effects occurring during decomposition of OM (Pessenda et al., 2004; Buso et al., 2013). The predominance of C3 plants during the Holocene at this site is corroborated by the work of others (Pessenda et al., 1996, 1998; Gouveia et al., 1999, 2002; Calegari, 2009; Coe, 2009; Chueng, 2012) on open forest vegetation in the Brazilian southeast region. Conversely, the E/Bt horizon is slightly enriched in ^{13}C ($\delta^{13}C = -19‰$), indicating a possible mixture of C3 and C4 plants. The difference, however, is not significant enough to indicate a strong shift of vegetation type.

4.3. Radiocarbon analyses

The resulting MRT ages of the total SOM samples and one humin fraction are reported both as conventional ^{14}C ages (Table 2) and as mean calendar ages (Fig. 6).

Several duplicates were produced for each horizon. The ^{14}C ages are quite variable within a single horizon (Table 2), and as expected they reflect a large variability of OM sources of different ages in this profile. The SOM chemical extraction applied removed only carbonates. In addition, the low carbon content in these soil horizons (<1.1%) limited us to break down the SOM fraction into its several active and passive carbon pools. Just one sample at KCCAMS, topsoil horizon A, was split into two aliquots to undergo SOM and humin extraction. Their ages are consistent with their respective fractions (i.e. the humin fraction is older than the SOM). Both age results are from the post-bomb era (e.g. ~1958 for UCIAMS113020 and 1956–1957 for UCIAMS113021, respectively), as they contain bomb ^{14}C from atmospheric nuclear weapon testing carried out in the north hemisphere during the 50s and 60s (Santos, 2012). For convenience, the two post-bomb values of horizon A are not shown in Fig. 6. These ^{14}C results are clearly from the very topmost topsoil layers, which typically receive continuous input of recent organic matter from plants and roots (Wang et al., 1996). Although these ages deviate from the LACUFF 11001 age result (30 ± 100 yrs BP) from the same horizon, one of them is still within 2σ of their uncertainties. In order to disclose the large variability of the ^{14}C dating results, we chose to calibrate the individual ^{14}C ages rather than averaging ^{14}C ages per horizon prior to calibration Although soil samples were homogenized prior to phytolith analyses, the material selected for ^{14}C dating was not. Nevertheless, the MRT results show a remarkable trend (Fig. 6) that appears to be a match between stratigraphy and age of soil formation, except for one result at horizon E, which is an inversion. Unfortunately, because these data are associated with total SOM rather than humin or charcoals, these ages should be interpreted as representing minimum ages and hence considered with caution (Pessenda et al., 2001).

From the MRT results, the studied soil profile appears to cover most of the Holocene, and therefore it should be important to inferring plaleoclimatic changes that have occurred in this small area of Atlantic Forest biome.

5. Discussion

To understand the complex past climate of the southeastern Brazilian region, researchers have based their investigations mostly on palynological studies (Ledru et al., 1998 and references therein). Only a few researchers have investigated the paleoenvironmental scenarios by incorporating phytoliths in their analyses (Alexandre et al., 1999; Borba-Roschel et al., 2006; Calegari, 2009; Coe, 2009).

Here, we used phytoliths in a multiproxy approach. We identified some general morphotypes (Fig. 4) and made use of the indices D/P, Bi and Iph of the phytolith assemblages recovered from the soil layers. In order to identify possible vegetation coverage changes through the Holocene, we then compared the indices calculated with those found for African phytolith studies in tropical regions that are similar to southeastern Brazil.

Alexandre et al. (1997b, 1999) have demonstrated that the proportion of globular granulate morphotypes produced by dicots, which are relatively resistant to dissolution in well drained and very weathered soils, versus morphotypes typical of grasses – the D/P index – can be useful for distinguishing forest from grassland and savannas. Here, the tree cover density D/P indices calculated for the soil profile (0.1 to 0.2) record conditions similar to those found in tropical Africa (Alexandre et al., 1997b; Barboni et al., 1999) and in a soil profile in Búzios, Rio de Janeiro, Brazil (Coe, 2009). The D/P values are lower than those found

Polylobate[d]	Trapeziform[d]	Cross[d]	Rondel[d]	Classified[e]	Unclassified[e]	D/P	Bi[d]	$\delta^{13}C$[f]	Coarse sand[d]	Fine sand[d]	Silt[d]	Clay[d]
0	2	0	4	72	28	0.1	74.5	− 24	65	22	9	5
0	1	0	3	63	37	0.1	81	− 23	67	20	9	5
0	1	0	5	60	40	0.1	75.6	− 19	62	22	9	7
0	2	0	3	51	49	0.2	64.5	− 22	27	9	10	54

by Alexandre et al. (1999) in a savanna area in Minas Gerais (MG), south-central Brazil (Table 1, Fig. 1).

The Bi (water stress) index is always very high (64 to 81%), like the values found by Coe (2009) in four soil profiles in Búzios (from 66 to 94%). The minimum Bi value is found in Zone I, indicating a reduction of the water stress conditions.

Our isotopic data coupled with the phytolith indices suggest that these conditions would be favorable to the development of vegetation with a mixture of C3 and C4 plants, with a predominance of C3 plants.

As mentioned earlier, the D/P and Bi indices help in defining the two delimitating zones (I and II) in the soil profile. Within these zones there were variations in phytolith stock and morphotypes (Figs. 4 and 5). In Zone I, there was an increase in the proportion of woody plant phytoliths and a decrease of the bulliform type, which can indicate a greater tree cover. The increase in tree density and the slight decrease of water stress seem to indicate a more humid environment during this period (at least until 6 cal ky BP). In Zone II (from 3 cal ky BP to the present), the vegetation cover exhibits no major variations, with a tree density slightly lower than that of Zone I. The Iph index also has its maximum value at the bottom of Zone II. Increased aridity probably limited the expansion of some dicotyledonous plants in this environment and promoted an increase in grassy openings.

The increase in phytoliths in Zone I may be explained by changes in grain size; an increase in the fine fraction would facilitate the accumulation of organic matter and phytoliths. This zone is represented by a textural horizon that would reinforce the hypothesis of accumulation for pedological causes. However, changes in the types of phytoliths and in the values of D/P and Bi indices could indicate variation in the vegetation or at least in the production of phytoliths. Because an increase occurs in the globular granulate morphotype, which is characteristic of eudicotyledonous plants that produce fewer phytoliths than Poaceae, this could have led to a decrease in total phytolith production. In addition, a decrease in the production of phytoliths did not necessarily mean a decrease in their stock, because the texture of the horizon favored the accumulation of phytoliths, potentially offsetting the reduction in their production.

The present findings, while preliminary, seem to be consistent with the work of Coe (2009) who used phytoliths to study the evolution of the vegetation of the Búzios/Cabo Frio region. Coe (2009) noticed that before 13 cal ky BP, there were no major changes in the type of

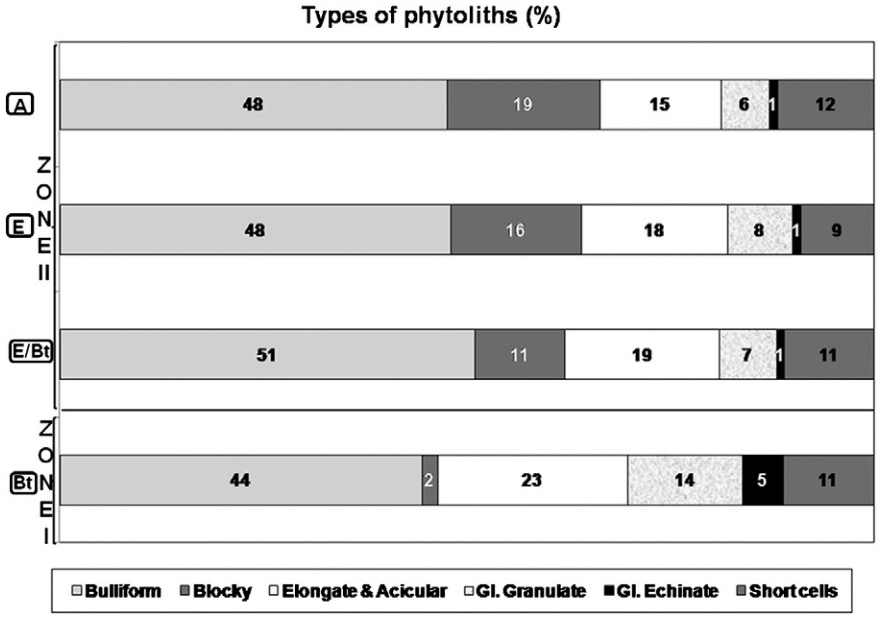

Fig. 4. Types of phytoliths (%).

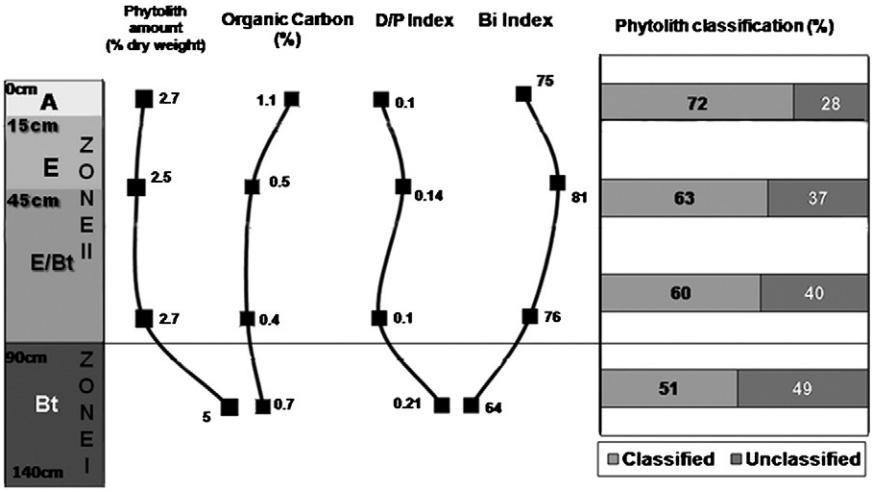

Fig. 5. Results of phytolith, and carbon content analyses of the studied soil profile.

vegetation (xeric forest). From 13 to 6 cal ky BP, the trend was an increase in tree cover, followed by a decrease from 6 to 1.5 cal ky BP. The lowest tree density period, which was associated with low D/P index values (0.2), ocurred between 6 and 5 cal ky BP. In addition to the low D/P index found for this period, less negative $\delta^{13}C$ values were also found, suggesting an opening of vegetation (grassy savanna). From 1.5 cal ky BP onwards, the phytolith signal no longer registered variations.

Alexandre et al. (1999), who also studied the phytolith assemblages in an oxisol on the boundary between rainforest and savanna in southeastern Brazil, found a savanna phase associated with a drier climate during the late Holocene (6.5 to 4.5 cal ky BP). This dry phase was followed by two periods represented by tree communities developed between ~4.5 and ~3 cal ky BP and around 900 cal ky BP that led to the formation of the present savanna/forest association.

Buso et al. (2013), who studied the Atlantic Forest biome at Espírito Santo (ES) (Fig. 1), southeastern Brazil using carbon isotopes and palynological analysis, also suggest the predominance of a humid period during midle Holocene (~7 to 4 cal ky BP) followed by a dry period from ~4 cal ky BP onwards. This change may be explained by the establishment of the modern position of the Intertropical Convergence Zone. This interpretation is in agreement with Ledru et al. (1998), who suggested that during this period polar air masses became largely restricted to southern latitudes, contributing to a cooling/drying phase. This change seems also to be in agreement with $\delta^{18}O$ from speleothems from southern and southeastern Brazil that indicate that during the mid- to late Holocene summer monsoons became more intense (Cruz et al., 2005, 2006). Furthermore, the establishment of modern climate conditions in South America by ~4 cal ky BP has also been postulated by Marchant and Hooghiemstra (2004), Wanner et al. (2008), and Wanner and Brönnimann (2012).

6. Conclusions

In this work we combined phytoliths and stable isotope analyses of soil samples with ^{14}C-AMS dates of SOM fractions from a soil profile collected in the region of Cabo Frio, on the southeast coast of Brazil. Those analyses were performed in order to infer the Holocene paleoclimate history of this region, which was completely occupied by the Atlantic Forest before the arrival of European colonists.

Phytolith and isotope analyses indicate the presence of open vegetation with few trees and predominance of C3 grasses from 3 cal ky BP to the present. Stable isotopic signatures of the soil profile confirm the predominance of C3 plants, except for E/Bt horizon that was less depleted

Table 2
The MRT ages of SOM from the four horizons are shown as ^{14}C. Laboratory identification numbers are provided for reference.

Samples	Sample size (mgC)	^{14}C age (yrs BP)	Cal BP (2 sigma)	Lab code
Horizon A				
A 1	0.80	$(0.3 \pm 1.0)\ 10^2$	281–present	LACUFF 11001
A 2	0.25	$(-5.35 \pm 0.15)\ 10^2$	(Post-bomb)	UCIAMS 113020
A 3 (humin)	0.025	$(-1.80 + 0.45)\ 10^2$	(Post-bomb)	UCIAMS 113021
Horizon E				
E	0.30	$(2.379 \pm 0.029)\ 10^3$	2459–2181	LACUFF 12070
Horizon E/Bt				
E/Bt 1	0.40	$(4.036 \pm 0.032)\ 10^3$	4567–4296	LACUFF 12069
E/Bt 2	1.10	$(2.72 \pm 0.12)\ 10^3$	3065–2365	LACUFF 11002
E/Bt 3	0.35	$(8.95 \pm 0.15)\ 10^2$	789–728	UCIAMS 113023
Horizon Bt				
Bt 1	0.66	$(8.81 \pm 0.18)\ 10^3$	10245–9459	LACUFF 11003
Bt 2	0.90	$(8.568 \pm 0.050)\ 10^3$	9551–9435	LACUFF 12068
Bt 3	0.58	$(5.520 \pm 0.020)\ 10^3$	6308–6207	UCIAMS 113022

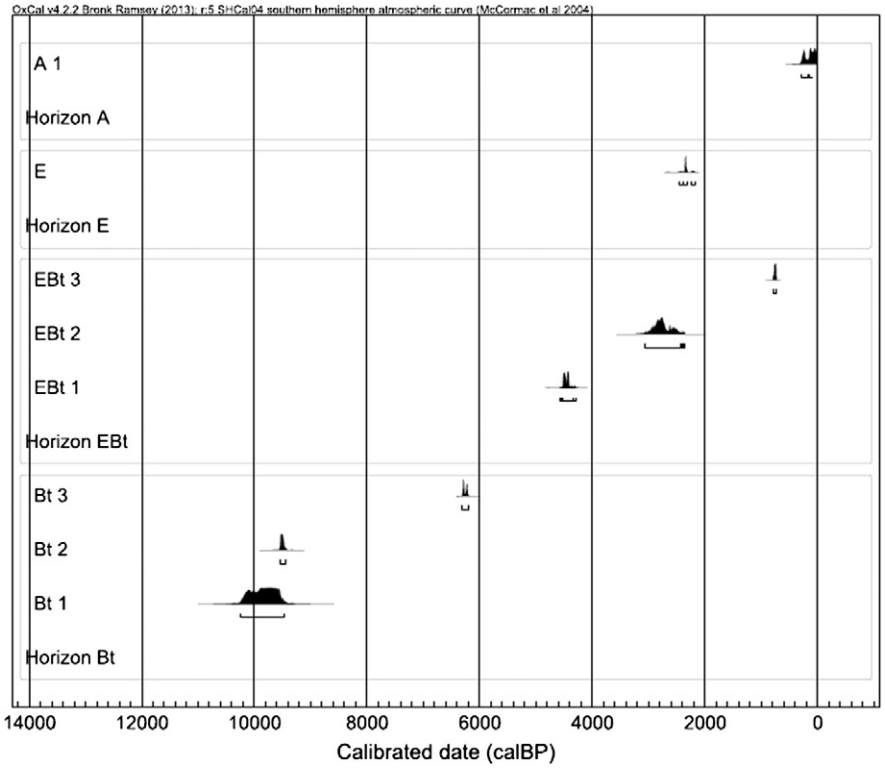

Fig. 6. Calibrated BP dates of each horizon. Note that the output of OxCal4 software package showing the calculated probability distribution of the event to have occurred between the considered periods.

in ^{13}C, indicating a shift towards more C4 vegetation. Moreover, the deepest horizon shows a greater D/P index, indicating a more humid environment in the first half of the Holocene (before 6 cal ky BP) than today. These findings, while preliminary, support previous research on pollen and phytoliths in southeastern Brazil that links drying/cooling conditions and vegetation shifts from woody plants to grassy openings.

Acknowledgments

The authors would like to thank the Brazilian funding agencies FINEP, CNPq, CAPES and FAPERJ for the financial support. We are grateful for Dr. Philip Meyers for the valuable comments and suggestions.

References

Alexandre, A., Meunier, J.D., Colin, F., Koud, J.M., 1997a. Plant impact on the biogeochemical cycle of silicon and related weathering processes. Geochim. Cosmochim. Acta 61, 677–682.

Alexandre, A., Meunier, J.D., Lezine, A.M., Vincens, A., Schwartz, D., 1997b. Phytoliths: indicators of grassland dynamics during the late Holocene in intertropical Africa. Palaeogeogr. Palaeoclimatol. Palaeoecol. 136, 213–229.

Alexandre, A., Meunier, J.D., Mariotti, A., Soubies, F., 1999. Late Holocene phytolith and carbon-isotope record from a latosol at Salitre, South-Central Brazil. Quat. Res. 51, 187–194.

Barboni, D., Bonnefille, R., Alexandre, A., Meunier, J.D., 1999. Phytoliths as paleoenvironmental indicators, West Side Middle Awash Valley, Ethiopia. Palaeogeogr. Palaeoclimatol. Palaeoecol. 152, 87–100.

Bement, L.C., Carter, B.J., Varney, R.A., Cummings, L.S., Sudbury, J.B., 2007. Paleoenvironmental reconstruction and bio-stratigraphy, Oklahoma Panhandle, USA. Quat. Int. 169–170, 39–50.

Beverly, R.K., Beaumont, W., Tauz, D., Ormsby, K.M., Von Reden, K.F., Santos, G.M., Southon, J.R., 2010. The Keck Carbon Cycle AMS Laboratory, University of California Irvine: status report. Radiocarbon 52 (2), 301–309.

Bidegain, P., 2005. Plano das Bacias Hidrográficas da Região dos Lagos e do rio São João. Rio de Janeiro. Consórcio Intermunicipal para Gestão das Bacias Hidrográficas da Região dos Lagos, Rio São João e Zona Costeira — CILSJ (153 pp.).

Borba-Roschel, M., Alexandre, A., Varajão, A.F.D.C., Meunier, J.D., Varajão, C.A.C., Colin, F., 2006. Phytoliths as indicators of pedogenesis and paleoenvironmental changes in the Brazilian cerrado. J. Geochem. Explor. 88, 172–176.

Borrelli, N., Osterrieth, M., Marcovecchio, J., 2006. Interrelations of vegetal cover, silicophytolith content and pedogenesis of typical argiudolls of the Pampean Plain, Argentina. Catena 75, 146–153.

Boutton, T.W., 1991. Stable carbon isotope ratios of natural materials. II. Atmospheric, terrestrial, marine and freshwater environments. In: Coleman, D.C., Fry, B. (Eds.), Carbon Isotope Techniques. Academic Press, New York, pp. 173–185.

Bremond, L., Alexandre, A., Hély, C., Guiot, J., 2005a. A phytolith index as a proxy of tree cover density in tropical areas: calibration with Leaf Area Index along a forest–savanna transect in southeastern Cameroon. Glob. Planet. Chang. 45, 277–293.

Bremond, L., Alexandre, A., Peyron, O., Guiot, J., 2005b. Grass water stress estimated from phytoliths in West Africa. J. Biogeogr. 32, 311–327.

Bronk Ramsey, C., 2009. Bayesian analysis of radiocarbon dates. Radiocarbon 51 (1), 337–360.

Buso, A.A., Pessenda, L.C.R., Oliveira, P.E., Giannini, P.C.F., Cohen, M.C.L., Volkmer-Ribeiro, C., Oliveira, S.M.B., Rossetti, D.F., Lorente, F.L., Filho, M.A.B., Schiavo, J.A., Bendassolli, J.A., França, M.C., Guimarães, J.T.F., Siqueira, G.S., 2013. Late Pleistocene and Holocene vegetation, climate dynamics, and Amazonian taxa in the Atlantic Forest, Linhares, SE Brazil. Radiocarbon 55, 1747–1762.

Calegari, M.R., 2009. Ocorrência e significado paleoambiental do Horizonte A húmico em Latossolos. Unpublished Doutorado thesis, Esalq, USP, 261p.

Chueng, K.F., 2012. Inferência da Cobertura Vegetal e das Condições Climáticas no Espinhaço Meridional, MG, durante o Quaternário, através dos Indicadores Fitólitos e Isótopos de Carbono. Unpublished Undergraduate monography, UERJ/FFP, São Gonçalo, p. 118.

Coe, H.H.G., 2009. Fitólitos como indicadores de mudanças na vegetação xeromórfica da região de Búzios/Cabo Frio, RJ, durante o Quaternário. Unpublished Doutorado thesis, Universidade Federal Fluminense.

Coe, H.H.G., Alexandre, A., Carvalho, C.N., Santos, G.M., Silva, A.S., Sousa, L.O.F., Lepsch, I.F., 2012. Changes in Holocene tree cover density in Cabo Frio (Rio de Janeiro, Brazil): evidence from soil phytolith assemblages. Quat. Int. http://dx.doi.org/10.1016/j.quaint.2012.02.044.

Consórcio Intermunicipal Lagos São João. http://www.micoleao.org.br/arquivos/mapas/uso_solo_sao_joao.jpg.

Cruz Jr., F.W., Burns, S.J., Karmann, I., Sharp, W.D., Vuille, M., Cardoso, A.O., Ferrari, J.A., Dias, P.L.S., Viana Jr., O., 2005. Insolation driven changes in atmospheric circulation over the past 116,000 years in subtropical Brazil. Nature 434 (7029), 63–66.

Cruz Jr., F.W., Burns, S.J., Karmann, I., Sharp, W.D., Vuille, M., 2006. Reconstruction of regional atmospheric circulation features during the late Pleistocene in subtropical Brazil from oxygen isotope composition of speleothems. Earth Planet. Sci. Lett. 248, 495–507.

Cunha, S.B., 1995. Impactos das obras de engenharia sobre o ambiente biofísico da Bacia do rio São João (Rio de Janeiro, Brasil), Rio de Janeiro.
Desjardins, T., Carneiro Filho, A., Mariotti, A., Chauvel, A., Girardin, C., 1996. Changes of the forest–savanna boundary in Brazilian Amazonia during the Holocene as revealed by soil organic carbon isotope ratios. Oecologia 108, 749–756.
Fredlund, G., Tieszen, L.L., 1994. Modern phytolith assemblages from the North American Great Plains. J. Biogeogr. 21, 321–335.
Gleixner, G., 2002. Molecular dynamics of organic matter in a cultivated soil. Org. Geochem. 3, 357–366.
Gordon, E.S., Goñi, M.A., 2003. Sources and distribution of terrigenous organic matter delivered by the Atchalaya River to sediments in the northern Gulf of Mexico. Geochim. Cosmochim. Acta 67.
Gouveia, S.E.M., Pessenda, L.C.R., Boulet, R., Aravena, R., Schell-Ybert, R., 1999. Isótopos do carbono dos carvões e da matéria orgcbeânica do solo em estudos de mudanças de vegetação e clima no Quaternário e da taxa de formação de solos do estado de São Paulo. An. Acad. Bras. Cienc. Rio de Janeiro 71 (4-II), 969–980.
Gouveia, S.E.M., Pessenda, L.C.R., Aravena, R., Boulet, R., Schell-Ybert, R., Bendassoli, J.A., Ribeiro, A.S., Freitas, H.A., 2002. Carbon isotopes in charcoal and soils in studies of paleovegetation and climate changes during the late Pleistocene and the Holocene in the southeast and centerwest regions of Brazil. Glob. Planet. Chang. Amsterdam 33 (1–2), 95–106.
Hedges, J.I., Parker, P.L., 1976. Land-derived organic matter in surface sediments from the Gulf of Mexico. Geochim. Cosmochim. Acta 40, 1019–1029.
Kelly, E.F., 1990. Method for extracting opal phytoliths from soil and plant material. Intern. Rep., Dep. Agron. Colorado State University. Fort Collins.
Kelly, E.F., Blecker, S.W., Yonker, C.M., Olson, C.G., Wohl, E.E., Todd, L.C., 1998. Stable isotope composition of soil organic matter and phytoliths as paleoenvironmental indicators. Geoderma 82, 59–81.
Killops, S., Killops, V., 2005. Introduction to Organic Geochemistry. Blackwell, Malden, MA.
Kondo, R., Childs, C., Atkinson, I., 1994. In: Zealand, L.C.N. (Ed.), Opal Phytoliths of New Zealand. Manaaki Whenua Press (85 pp.).
Krauss, D.A., Kaplan, L., Strauss, E., 1997. The use of phytolith analysis in paleoenvironmental reconstruction and environmental management; a case study on Martha's Vineyard, MA. Proceedings of the Twenty-Fourth Annual Conference on Ecosystems Restoration and Creation: May 1997, pp. 116–131.
Ledru, M.P., Salgado-Labouriau, M.L., Lorscheitter, M.L., 1998. Vegetation dynamics in Southern and Central Brazil during the last 10,000 yr. BP. Rev. Palaeobot. Palynol. 99, 131–142.
Madella, M., Alexandre, A., Ball, T., 2005. International code for phytolith nomenclature 1.0. Ann. Bot. 96, 253–260.
Marchant, R., Hooghiemstra, H., 2004. Rapid environmental change in African and South American tropics around 4000 years before present: a review. Earth Sci. Rev. 66, 217–260.
Martin, C.W., Johnson, W.C., 1995. Variation in radiocarbon ages of soil organic matter fractions from late Quaternary buried soils. Quat. Res. 43 (2), 232–237.
Martinelli, L.A., Ometto, J.P.H.B., Ferraz, E.S., Victoria, R.L., Camargo, P.B., Moreira, M.Z., 2009. Desvendando Questões Ambientais com Isótopos Estáveis. Oficina de Textos, São Paulo.
McCormac, F.G., Hogg, A.G., Blackwell, P.G., Buck, C.E., Higham, T.F.G., Reimer, P.J., 2004. SHCal04 Southern Hemisphere Calibration, 0–11.0 cal kyr BP. Radiocarbon 46 (3), 1087–1092.
Mercader, J., Bennett, T., Esselmont, C., Simpson, S., Walde, D., 2009. Phytoliths in woody plants from the Miombo woodlands of Mozambique. Ann. Bot. 104, 91–113.
Messager, E., Lebreton, V., Marquer, L., Russo-Ermolli, E., Orain, R., Renault Miskovsky, J., Lordkipanidze, D., Despriée, J., Peretto, C., Arzarello, M., 2010. Palaeoenvironments of early hominins in temperate and Mediterranean Eurasia: new palaeobotanical data from Palaeolithic key-sites and synchronous natural sequences. Quat. Sci. Rev. 1–9.
Mulholland, S.C., 1989. Phytoliths shape frequencies in North Dakota grasses: a comparison to general patterns. J. Archaeol. Sci. 489–511.
Pessenda, L.R.C., Aravena, R., Melfi, A.J., Telles, E.C.C., Boulet, R., Valencia, E.P.E., Tomazello, M., 1996. The use of carbon isotopes (C-13, C-14) in soil to evaluate vegetation changes during the Holocene in Central Brazil. Radiocarbon New Haven 38 (2), 191–201.
Pessenda, L.R.C., Gouveia, S.E.M., Aravena, R., Gomes, B.M., Boulet, R., Ribeiro, A.S., 1998. Radiocarbon dating and stable carbon isotopes of soil organic matter in forest–savanna boundary areas in the southern Brazilian Amazon forest. Radiocarbon New Haven 40 (2), 1013–1022.
Pessenda, L.R.C., Gouveia, S.E.M., Aravena, R., 2001. Radiocarbon 43 (2B), 595–601.
Pessenda, L.R.C., Ribeiro, A.S., Gouveia, S.E.M., Aravena, R., Boulet, R., Bendassolli, J.A., 2004. Vegetation dynamics during the late Pleistocene in the Barreirinhas region, Maranhão State, northeastern Brazil, based on carbon isotopes in soil organic matter. Quat. Res. San Diego 62, 183–193.
Piperno, D., 1988. Phytoliths Analysis: An Archaeological and Geological Perspective. Academic Press, San Diego.
Primo, P., Volker, C.M., 2003. Bacias hidrográficas dos rios São João e das Ostras: águas, terras e conservação ambiental. Consórcio Intermunicipal Lagos São João, Rio de Janeiro.
Quintela, M.A., Cunha, S.B., 1990. Regime pluviométrico e diagnóstico ambiental na área de influência do reservatório de Juturnaíba, RJ. Anuário do Instituto de GeociênciasUniversidade Federal do Rio de Janeiro 164–182 (1987–1988).
Santos, G.M., 2012. Beyond archaeology: ^{14}C-AMS and the global carbon cycle. The IX Latin American Symposium on Nuclear Physics and Applications, American Institute of Physics—AIP Conf. Proc. , 1423, pp. 311–318. http://dx.doi.org/10.1063/1.3688819.
Santos, G.M., Ormsby, K., 2014. Behavioral variability in ABA chemical pretreatment close to the 14C age limit. Radiocarbon 55 (3–4) (in press).
Santos, G.M., Southon, J.R., Griffin, S., Beaupre, S.R., Druffel, E.R.M., 2007a. Ultra small-mass AMS ^{14}C sample preparation and analyses at KCCAMS/UCI Facility. Nucl. Inst. Methods Phys. Res. B 259, 293–302.
Santos, G.M., Moore, R.B., Southon, J.R., Griffin, S., Hinger, E., Zhang, D., 2007b. AMS ^{14}C sample preparation at the KCCAMS/UCI Facility: status report and performance of small samples. Radiocarbon 49 (2), 255–269.
Saraiva, V.I.C. 2012. Análise da Suscetibilidade à Erosão Laminar dos Solos da Bacia Hidrográfica dos Lagos e São João. Unpublished Graduate monography, UERJ, Rio de Janeiro, Brazil.
Sedov, S., Solleiro-Rebolledo, E., Morales-Puente, P., Arias-Herreìa, A., Vallejo-Gòmez, E., Jasso-Castañeda, C., 2003. Mineral and organic components of the buried paleosols of the Nevado de Toluca, Central Mexico as indicators of paleoenvironments and soil evolution. Quat. Int. 106–107, 169–184.
Strömberg, C.A.E., 2004. Using phytolith assemblages to reconstruct the origin and spread of grass-dominated habitats in the great plains of North America during the late Eocene to early Miocene. Palaeogeogr. Palaeoclimatol. Palaeoecol. 207, 239–275.
Tapia, E.M., Solleiro-Rebolledo, E., Gama-Castro, J., Villalpando, J.L., Sedov, S., 2003. Paleosols in the Teotihuacan valley, Mexico: evidence for paleoenvironment and human impact. Rev. Mex. Cienc. Geol. 20, 270–282.
Twiss, P.C., 1992. Predicted world distribution of C3 and C4 grass phytoliths. In: Mulholland, S.C. (Ed.), Phytoliths Systematics: Emerging Issues. Advance Archaeological Museum Science, vol. 1. Plenum Press, New York, pp. 113–128.
Twiss, P.C., Suess, E., Smith, R.M., 1969. Morphological classification of grass phytoliths. Procedure of Soil Sci. Soc. Am, pp. 109–115.
Wang, Y., Amundson, R., Trumbore, S., 1996. Radiocarbon dating of soil organic matter. Quat. Res. 45, 282–288.
Wanner, H., Brönnimann, S., 2012. Is there a global Holocene climate mode? PAGES News, 20(1), pp. 44–45.
Wanner, H., Beer, J., Bütikofer, J., Crowley, T.J., Cubasch, U., Flückiger, J., Goose, H., Grosjean, M., Joos, F., Kaplan, J.O., Küttel, M., Müller, S.A., Prentice, I.C., Solomina, O., Stocker, T.F., Tarasov, P., Wagner, M., Widmann, M., 2008. Mid to Late Holocene climate change: an overview. Quat. Sci. Rev. 27, 1791–1828.
Xu, X., Trumbore, S.E., Zheng, S., Southon, J.R., McDuffee, K.E., Luttgen, M., Liu, J.C., 2007. Modifying a sealed tube zinc reduction method for preparation of AMS graphite targets: reducing background and attaining high precision. Nucl. Inst. Methods Phys. Res. B 259, 320–329.